INTEGRATED HTS CCT MAGNET AND BEAM PIPE : A PROPOSAL FOR THE FCC-ee FINAL FOCUS QUADRUPOLE QC1L/R1

M. Marchand*, L. Brunetti, G. Lamanna, M. Le Garrec, CNRS/IN2P3-LAPP, Annecy, France
F. Bardi, M. Koratzinos, CERN, Geneva, Switzerland
F. Toussaint, SYMME-USMB, Annecy, France
M. Duda, PSI Center for Accelerator Science and Engineering, Villigen, Switzerland

Abstract

High Temperature Superconductors (HTS) and Canted Cosine Theta (CCT) technologies have been extensively studied in recent years, particularly for high-field accelerator magnets. Their application to next-generation particle accelerators is especially promising. This article presents the combination of these two technologies for the FCC-ee Final Focus (FF) quadrupole QC1L/R1, including its integration within the Machine-Detector Interface (MDI).

We detail the specific design, mechanical specifications, and manufacturing process—driven by the coil's significant curvature angle—as well as the cryogenic test strategy and results. Additionally, we describe the design of a cooled beam pipe adapted to the magnet and cryostat constraints.

INTRODUCTION

The Future Circular Collider (FCC) will operate as a Higgs and electroweak factory, colliding positron and electron beams at high energy (FCC-ee) [1]. The particles are guided and focused by magnets throughout the collider, particularly near the Interaction Point (IP) within the MDI. The design of these FF quadrupole magnets is a critical challenge for the feasibility of FCC-ee.

The current baseline magnet technology for the FCC-ee MDI [2,3] uses conventional NbTi superconducting magnets. However, to address the demands of next-generation particle accelerators [4], several research teams have explored advanced technologies, such as direct-winded magnets [5–8] and other alternative solutions [9–12]. This work focuses on the FF quadrupoles for the MDI, with particular emphasis on QC1L/R1[1], the optical element closest to the IP, where the stakes are highest [13]. Our proposed solution combines two promising approaches: HTS tapes [14, 15] and CCT winding [16–18]. This combination optimizes the high-precision magnetic field, stress distribution in the coils, compactness, sustainability, and design flexibility.

This article outlines the demonstrator strategy, focusing on the development of the first prototype. We detail the magnetic field design, magnet specifications, and the manufacturing process for machining highly specific parts, including the complex groove design within a confined space and the stringent tolerances required. We also present cryogenic test results to evaluate the superconducting properties of various HTS tapes under severe bending and symmetrical angle constraints. The goal is to select the most suitable supplier based on critical current performance, manufacturability, and cost.

Furthermore, we describe the beam pipe design, adapted for integration within the cryostat, along with numerical simulations and prototype manufacturing in preparation for preliminary tests.

* matthieu.marchand@lapp.in2p3.fr

THE FINAL FOCUS HTS CCT QUADRUPOLE

Before developing a full-scale HTS CCT QC1L/R1 prototype and measuring its magnetic field, we must validate the mechanical feasibility and superconducting efficiency of the conductor, despite the stringent magnetic and mechanical specifications. Selecting the appropriate conductor is paramount.

Design and Manufacturing

The primary objective of the FCC-ee QC1L/R1 quadrupole is to generate a highly precise magnetic field to focus the particle beams at the IP, ensuring the desired luminosity. Magnetic simulations define the quadrupole field, which in turn determines the CCT coil shape (Fig. 1a). The mechanical specifications are then derived from this design.

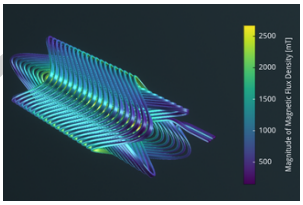

(a) QC1L/R1 Magnetic design and shape of CCT coil.

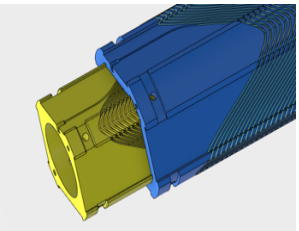

(b) QC1L/R1 design : a 2-layer magnet.

Figure 1: Overview of QC1L/R1 magnetic and mechanical design.

The final magnet will consist of two CCT layers, each with an opposed and canted groove carved into an aluminum body (Fig. 1b). To achieve a 3.2 T field, the HTS coil, shaped as a 4 mm square tape is inserted into the tortuous groove.

The 700 mm-long magnet with a 40 mm aperture presents a major mechanical challenge: ensuring the spatial precision of the coil. The 123 turns of the 4 mm-deep groove must

[1] QC1L/R1 is the designation of the last quadrupole before IP in the z Lattice. QD0A is its designation in the LCC Lattice

be machined with a ±60° tilt and a stringent thickness tolerance of +0.03 mm. Only a few suppliers possess the 5-axis machining capabilities required for this task. All QC1L/R1 parameters are presented in Table 1.

Table 1: QC1L/R1 Parameters

Parameters	Unit	Value
Technology	-	HTS and CCT
Magnetic Field	T	3.2
Field gradient	T/m	100
Magnetic Length	mm	700
Aperture	mm	40
No. of Winding Turn	-	123
Distance Between Turns	mm	1.1
Radial Spar Thickness	mm	2
Between-layer radial thickness	mm	0.1
Groove Dimensions	mm	0.163 × 4
Tilt angle	°	±60
Groove Tolerance	mm	+0.03
Number of Conductors	-	10
Min. Radius of curvature	mm	3.55

To demonstrate the fabrication process, we manufactured reduced single-layer prototypes (80 mm long, with a 3-turn groove) (Fig. 2a). Additionally, since smaller bending radii reduce the nominal current [19, 20], we must test the behavior of different HTS tapes under these specific design and winding conditions using the small prototype.

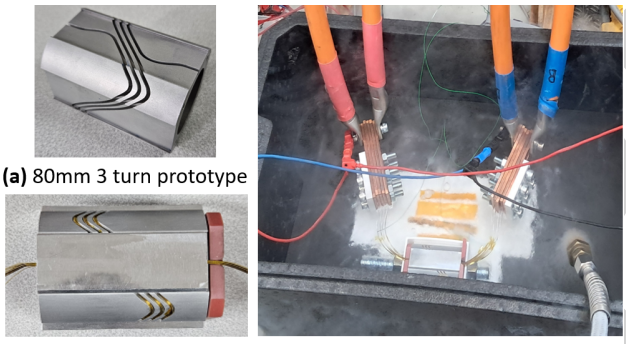

(a) 80mm 3 turn prototype

(b) Winded prototype

(c) Test setup in a N_2 bath

Figure 2: QC1L1 prototype through its different steps of test.

Winding and Test Results

Based on many comparative tests in this field [21–24] and the specifications of global suppliers, we selected three HTS tapes with distinct parameters, presented in Table 2.

For a 0.1 mm-thick multilayer tape, any unadapted manipulation could damage the extremely sensitive micron-thick superconducting layer on its substrate. In consequence, we developed a semi-automatic winding bench and specialized tools to handle this critical assembly step prior to testing. A winded prototype with SST tape is shown in Figure 2b.

[3] Resin reinforced with fiberglass to sustain thermic deformation during cryogenic tests

[3] Based on numerical simulations

Table 2: Selected Conductor Characteristics

Parameters	FFJ	SST	AMPeers
Origin	Japan	China	U.S.A
Configuration	Double	Single	Single
Insulation	None	Yes (50 µm)	None
Dimensions	0.1×4mm	0.1 × 4mm	0.07×2mm
Former mater.	Al6063	Al6063	Onyx[2]
I_C (at 77K)	318 A	200 A	90 A
Expected[3] I_C	290 A	160 A	90 A

To evaluate each conductor's efficiency, we tested multiple configurations with varying numbers of HTS tapes : from 1 to 4 for the FFJ [25], 1 to 8 for SST [26] and 2 for the AMPeers [27], all powered in parallel. The setup, shown in Figure 2c, was immersed in a nitrogen bath at 77 K. The tapes were powered, at a rate of 10 A/s in 50 A increments, until reaching the critical current I_C, defined as the point where the voltage drop reaches 1µV/cm. These tests were performed at the Paul Scherrer Institute (PSI).

Figure 3 shows the voltage µV as a function of current A for a single SST tape in a 3-turn prototype. The critical current I_C, reached at a 100 µV threshold, is measured at 141 A for a magnetic field estimated at 36 mT (numeric simulations). Extrapolating to the final QC1L/R1 magnet (peak field of 3.2 T at the conductor), the magnet specifications would be easily met using a stack of 12 such tapes operated at 4.5 K.

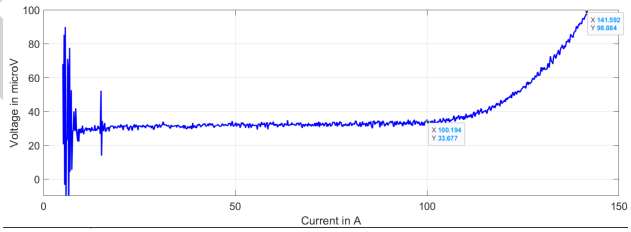

Figure 3: Voltage µV as a function of current A, for a single SST tape at 77 K.

Considering strategic parameters — such as critical current, tape width, insulation for future serial cabling, cost, and lead times — the SST tape emerges as the most suitable option for the future magnet prototype. The tape, produced by the Chinese supplier, offers high critical current efficiency, ready availability in bulk, and flexibility in width to adapt to potential magnet design adjustments.

Prospective

Based on the initial cryogenic test results, the SST tape is the most promising candidate for a full-scale QC1L/R1 demonstrator. The next step involves building a complete two-layer quadrupole with a 20-turn groove and a configuration of multiple SST tapes in series. This will allow us to study the two-layer CCT magnet magnetic field and its impact on critical current.

THE BEAM PIPE

The integration of a HTS CCT version of QC1L/R1 within the FCC-ee cryostat directly affects the design of nearby components, particularly the beam pipe.

Design and Specifications

The 40 mm magnet aperture and the 30 mm inner diameter of the beam pipe (fixed by the physics) leave only 5 mm radial space for the beam pipe wall, the magnet's thermal insulation, and the beam pipe cooling system, which must evacuate heat generated by particle beam radiation (Fig. 4a). Additionally, the LumiCal near the IP [13] restricts access to cooling fluid in the immediate vicinity of the IP. Thus, the inlet and outlet for thermal regulation must be located outside the MDI region. These constraints directly influence the beam pipe design and introduce several challenges.

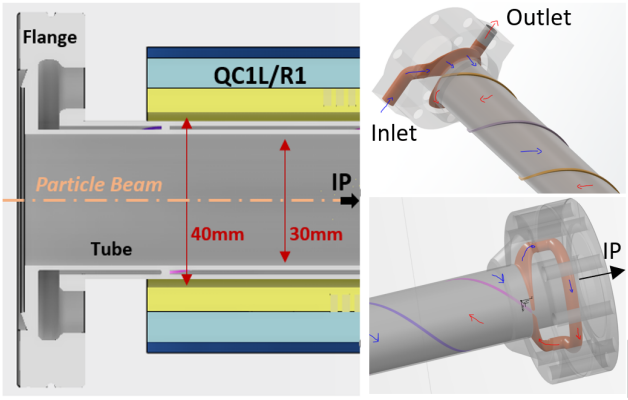

(a) Beam pipe integration and dimensional specifications

(b) Representation of water flow inside the hollow wall and the flange's channels

Figure 4: Overview of Beam Pipe Design.

The 3 m-long beam pipe is designed first to cool the tube using an internal double-spiral structure between two walls. The flanges incorporate internal channels to collect and guide the calorific fluid, currently defined as simple water, from the inlet to the outlet (Fig. 4b). The design ensures smooth fluid flow to minimize turbulence and vibrations [28], with the fluid circulating around the tube and using the flanges to reverse direction, thereby cooling the entire structure.

Numerical Simulations and Manufacturing

To validate the design from thermal, fluid dynamics and vibration perspectives, we performed numerical simulations. They are presented in Table 3.

The simulations confirm that a 20 °C water flow efficiently cools the tube, preventing the temperature from exceeding 23 °C while maintaining acceptable pressure levels. The smooth internal channels limit the maximum water velocity to minimize turbulence and vibrations. Additionally, the beam pipe structure is sufficiently sturdy to prevent mechanical deformation and buckling.

Table 3: Beam Pipe Numerical Simulation Results

General Parameters			
Material	316L	Length	3 m
Int. diameter	30 mm	Ext. diameter	36 mm
Wall thick.	1 mm	Water thick.	1 mm
Input Parameters		**Simulation results**	
Heated Surface	100 W/m	Pipe Max T°	23 °C
Mass Flow Rate	0,024 Kg/s	Max Deform.	0.6 mm
Internal Vacuum	100 Pa	Max Stress	34 MPa
Ultra Vacuum	10-7 Pa	First Mode	23 Hz
Fluid Pres.	0,18 MPa	Max H_2O Press.	1.8 bar
Inlet H_2O T°	20 °C	Outlet H_2O T°	21.5 °C
Inlet H_2O v	0.5 m/s	Max v	1.5 m/s

Manufacturing the 3 m beam pipe presents its own challenges. The tube consists of two parts: the inner tube machined to directly integrate the spiral structure, and the outer tube, adjusted and assembled to the first one. However, the flanges, with their complex internal channels, are 3D-printed in metal and precisely welded to the tube to avoid pressure leaks.

Prospective

With the design validated by simulations, the next step is experimental verification. The first flange has already been 3D-printed in metal at the SYMME laboratory. It will be mounted on a 1 m tube prototype, along with a second flange. A dedicated test bench will measure the real thermal, fluid dynamics, and vibration characteristics of the prototype, as well as its compatibility with the future full-scale quadrupole prototype.

CONCLUSION

QC1L/R1 is a critical element of FCC-ee, and this study demonstrates that the application of HTS and CCT technologies is a viable and promising option for its design. The manufacturing process has been validated through the fabrication of a first 3-turn prototype, and the cryogenic tests confirm the compatibility of the design with the SST tape. Despite the severe bending radius imposed by the CCT geometry, the tape exhibits promising superconducting properties. Furthermore, the beam pipe's specific design meets the thermal and mechanical specifications, as confirmed by numerical simulations.

Future work will focus on developing a complete Final Focus quadrupole, mounted on a 1 m beam pipe, to validate the magnetic field quality and optimize the overall design.

ACKNOWLEDGMENT

The authors wish to thank PSI and its technical staff for conducting the cryogenic tests using their facilities, as well as the FCC-ee MDI collaboration for their support and interest in this project. We also acknowledge Ampeers and SST for providing the HTS tapes free of charge. The winding method is patented (EP4449455) and used with permission.

REFERENCES

[1] A. Abada *et al.*, "FCC-ee: the lepton collider", *Eur. Phys. J. Spec. Top.*, vol. 228, pp. 261–623, 2019. doi:10.1140/epjst/e2019-900045-4

[2] M. Benedikt *et al.*, "Future circular collider feasibility study report: volume 1, physics, experiments, detectors", *Eur. Phys. J. C*, vol. 85, no. 1468, Dec. 2025. doi:10.17181/CERN.9DKX.TDH9

[3] M. Benedikt *et al.*, "Future circular collider feasibility study report: volume 2, accelerators, technical infrastructure and safety", *Eur. Phys. J. C*, vol. 234, pp. 5713–6197, Nov. 2025. doi:10.17181/CERN.EBAY.7W4X

[4] M. Benedikt *et al.*, "Future circular collider feasibility study report: volume 3, civil engineering, implementation and sustainability", *Eur. Phys. J. C*, vol. 234, no. 17, pp.5113-5383, Oct. 2025. doi:10.17181/CERN.I26X.V4VF

[5] B.Parker *et al.*, "Compact superconducting final focus magnet options for the ILC", in *Proc. PAC'05*, Knoxville, TN, USA, May 2005, paper RPPP017, pp. 1569–1571. doi:10.1109/PAC.2005.1590838

[6] B.Parker *et al.*, "BNL direct wind superconducting magnets", *IEE Trans. Appl. Supercond.*, vol. 22, no. 3, pp. 4101604-4101604, June 2012. doi:10.1109/TASC.2011.2175693

[7] M. Anerella *et al.*, "Design and construction of a superconducting "direct wind" R&D magnet for the EIC interaction region", *IEEE Trans. Appl. Supercond.*, vol. 36, no. 3, pp. 1-4, May 2026. doi:10.1109/TASC.2026.3658299

[8] M. Kumar*et al.*, "Test results for the high field direct wind magnet", *IEEE Trans. Appl. Supercond.*, vol. 36, no. 3, pp. 1-5, May 2026. doi:10.1109/TASC.2025.3615558

[9] C. Martins Jardim *et al.*, "PRISMAC: a R&D program and a new dedicated laboratory for very high field superconducting magnets", *IEEE Trans. Appl. Supercond.*, vol. 36, no. 3, pp. 1-5, May 2026. doi:10.1109/TASC.2025.3628286

[10] A. Thabuis *et al.*, "The first superconducting final focus quadrupole prototype of the FCC-ee study", in *Proc. IPAC 2024*, Nashville, TN, United States, May 2024, pp.WEPS65 doi:10.18429/JACoW-IPAC2024-WEPS65

[11] M. D'Addazio *et al.*, "Conceptual structural design and analysis of a 20 T hybrid *Cosθ* dipole for future particle colliders", *IEEE Trans. Appl. Supercond.*, vol. 35, no. 5, pp. 1-5, Aug. 2025. doi:10.1109/TASC.2024.3513274

[12] S. Busatto *et al.*, "HTS superferric combined function magnet for the FCC-ee project", *IEEE Trans. Appl. Supercond.*, vol. 36, no. 3, pp. 1-5, May 2026. doi:10.1109/TASC.2025.3628302

[13] M.Boscolo *et al.*, "Status of the FCC-ee interaction region design", *EPJ Techn. Instrum.*, vol. 12, no. 4, Aug. 2025. doi:10.1140/epjti/s40485-025-00117-3

[14] J. Georg Bednorz and K. Alex Müller, "Perovskite-type oxides - The new approach to high-T_c, superconductivity", *IBM J. Res. Dev.*, vol. 33, no. 3, May 1989. doi:10.1147/rd.333.0199

[15] T. Shen and L. Garcia Fajardo, "Superconducting accelerator magnets based on high-temperature superconducting Bi-2212 round wires", *Instruments* , vol. 4, no. 2, pp. 17, Jun. 2020. doi:10.3390/instruments4020017

[16] D.I. Meyer and R. Flasck, "A new configuration for a dipole magnet for use in high energy physics applications", *Nucl. Instrum. Methods*, vol. 80, no. 2, 1970. doi:10.1016/0029-554x(70)90784-6

[17] R. B. Meinke, M. J. Ball, C. L. Goodzeit, "Superconducting double-helix accelerator magnets", in *Proc. PAC'03*, Portland, OR, USA, May 2003, pp. 1996–1998. doi:10.1109/PAC.2003.1288752

[18] S. Caspi *et al.*, "Canted–cosine–theta magnet (CCT) — A concept for high field accelerator magnets", *IEEE Trans. Appl. Supercond.*, vol. 24, no. 3, Jun. 2014. doi:10.1109/TASC.2013.2284722

[19] G. Celentano *et al.*, "Bending behavior of HTS stacked tapes in a cable-in-conduit conductor with twisted al-slotted core", *IEEE Trans. Appl. Supercond.*, vol. 29, no. 5, Aug. 2019. doi:10.1109/TASC.2019.2899248

[20] H. Ye *et al.*, "Bending characteristics of multi-layer spiral HTS cable with large tape gap", *Physica C*, vol. 632, no. 1354691, May 2025. doi:10.1016/0029-554X(70)90784-6

[21] T. Yang, W. Li and Y. Xin, "Comparative study of current carrying capacity between 1G and 2G HTS tape samples at different temperatures and magnetic fields", *Phys. Scr.*, vol. 99, no. 3, Mar. 2024. doi:10.1088/1402-4896/ad2044

[22] J. Shimoyama, T. Motoki, "Current status of high temperature superconducting materials and their various applications", *IEEJ Trans. Electr. Electron. Eng.*, vol. 19, no. 3, Dec. 2025. doi:10.10.1002/tee.23976

[23] D Uglietti, "A review of commercial high temperature superconducting materials for large magnets: from wires and tapes to cables and conductors", *Supercond. Sci. Technol.*, Vol. 32, No. 5, Apr. 2019. doi:10.1088/1361-6668/ab06a2

[24] S. Kar *et al.*, "Optimum copper stabilizer thickness for symmetric tape round (STAR) REBCO wires with superior mechanical properties for accelerator magnet applications", *IEEE Trans. Appl. Supercond.*, vol. 29, no. 5, Aug. 2019. doi:110.1109/TASC.2019.2912312

[25] Faraday Factory Japan LLC, https://www.faradaygroup.com/en

[26] Shanghai Superconductor Technology Co., https://www.shsctec.com/en

[27] AMPeer, https://www.ampeers.com/n

[28] M.Marchand *et al.*, "FCC-ee HTS CCT magnet design proposal for the final focus quadrupole and its cooled beam pipe", in *Proc. FCC Physics Workshop*, Jan. 2026.